Reaction $^{27}Al(\alpha,d)^{29}Si$ at 27.2 MeV

L. C. Bland and H. T. Fortune
Physics Department, University of Pennsylvania, Philadelphia, Pennsylvania 19104

O. K. Gorpinich, Yu S. Stryuk, and V. N. Shcherbin
Institute of Nuclear Research, Academy of Science of the Ukrainian SSR, Kiev, Union of Soviet Socialist Republic

V. V. Tokarevski*
Physics Department, Swarthmore College, Swarthmore, Pennsylvania 19081

(Received 26 July 1979)

At a bombarding energy of 27.2 MeV, complete angular distributions have been measured for the reaction $^{27}Al(\alpha,d)^{29}Si$, populating the seven lowest states of ^{29}Si. Data have been analyzed in distorted-wave Born approximation, using both cluster and microscopic formalisms. For the latter, transfer amplitudes were taken from shell-model and weak-coupling calculations.

[NUCLEAR REACTION $^{27}Al(\alpha,d)$; $E=27.2$ MeV; measured $\sigma(E_d,\theta)$, $\theta=3$–$169°$ ^{29}Si levels. DWBA analysis, microscopic and macroscopic.]

I. INTRODUCTION

The reaction $^{27}Al(\alpha,d)^{29}Si$ has previously been studied at bombarding energies of 28.4 MeV[1] and 18.7 MeV,[2] but data are sparse. At the higher energy, measurements were performed for only four angles in the range 23°–55° (lab). In Ref. 2, the angular range was large enough but data were obtained for only the ground and first excited state.

The present report concerns an investigation of this reaction at a bombarding energy of 27.2 MeV and includes data for the first seven states of ^{29}Si for an angular range of 9°–169°, with additional measurements at more forward angles for a few states. A spectrum is displayed in Fig. 1. Preliminary experimental results have been published elsewhere[3]; differential cross sections are tabulated in Ref. 4. Data have been analyzed in the framework of distorted-wave Born approximation (DWBA) using both microscopic and macroscopic formalisms.

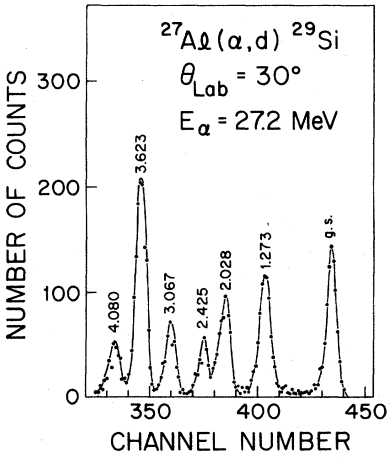

FIG. 1. Spectrum of the reaction $^{27}Al(\alpha,d)^{29}Si$, at a bombarding energy of 27.2 MeV and a laboratory angle of 30°.

II. EXPERIMENTAL PROCEDURE AND RESULTS

The measurement of the differential cross sections was carried out at the R-7 cyclotron of the Institute of Nuclear Research in Kiev. The geometry of the experiment, monitoring technique of the incident beam, and the method of absolute cross

TABLE I. Results of $^{27}Al(\alpha,d)^{29}Si$.

E_x (MeV)	J^π	σ (mb) 10°–90°(c.m.)	σ (mb) 90°–160°(c.m.)	L	S_L [a]
0	$\frac{1}{2}^+$	0.33	0.084	2	4.3
				4	~0
1.27	$\frac{3}{2}^+$	0.41	0.091	0	0.90
				2	1.6
				4	0.44
2.03	$\frac{5}{2}^+$	0.28	0.099	2	0.48
				4	2.8
2.43	$\frac{3}{2}^+$	0.19	0.058	2	0.7
				4	2.7
3.07	$\frac{5}{2}^+$	0.12	0.075	0	0.41
				2	0.89
				4	0.31
3.62	$\frac{7}{2}^-$	0.60	0.25	1	0.25
				3	0.10
				5	0.48
4.08	$\frac{7}{2}^+$	0.20	0.13	0	~0
				2	0.70
				4	1.2

[a] $S_L \propto \sigma_{exp}/\sigma_{calc}$, with bound-state parameters $r_0=1.175$, $a=0.40$.

section determination are identical to those which were published earlier.[5] The deuterons from the reaction ^{27}Al$(\alpha,d)^{29}$Si were detected by a set of ΔE-E Si(Li) counter telescopes. The thickness of the ΔE detectors was about 200 μm and the thickness of the E detectors about 1500 μm. At angles less than 60° (lab) Ta or Mo absorbers were placed before the ΔE detectors to cut off the elastically scattered alphas.

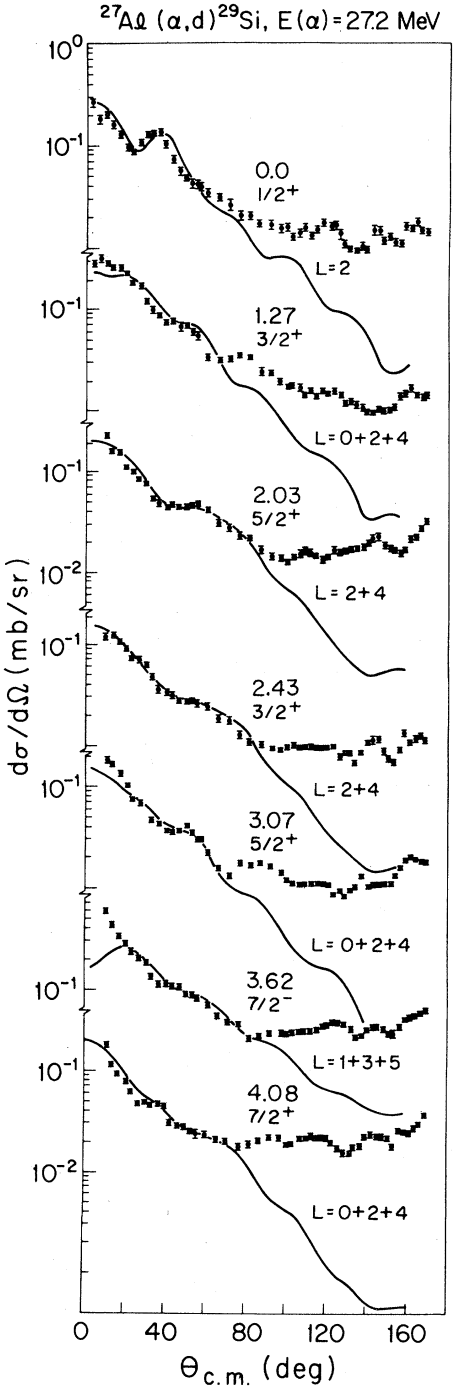

FIG. 2. Experimental angular distributions for ^{27}Al$(\alpha,d)^{29}$Si compared with cluster-transfer DWBA curves calculated using optical-model and bound-state parameter set K listed in Table II. Admixtures of different L values are listed in Table I.

Angular distributions were measured in 3° steps in the angular range of 3°–169° (lab) for the ground state and first excited state, and from 9°–169° for other levels. Spins and parities of these states are listed in Table I. Experimental angular distributions are displayed in Fig. 2. The experimental errors are the weighted mean values of the statistical errors of several measurements. The uncertainty in the absolute cross section is ≈7%.

Two features of the experimental angular distributions are immediately apparent. All angular distributions are forward peaked, indicative of a direct reaction mechanism. However, with increasing excitation energy the ratio of backward to forward angle cross sections increases as illustrated by comparing the angle-integrated cross sections from 10°–90° (c.m.) and 90°–160° (c.m.) (Table I). Another feature of the angular distributions is their rather smooth oscillatory structure at both forward and back angles.

III. ANALYSIS

Experimental angular distributions were first analyzed with the assumption that the (α,d) reaction proceeds by the transfer of a proton-neutron correlated pair, i.e., a quasideuteron cluster. Neglecting the spin-orbit interaction in the exit channel the theoretical cross section may be written as[6]

$$\frac{d\sigma}{d\Omega}=\frac{2J_B+1}{2J_A+1}\sum_{LSJ}|A_{LSJ}|^2\sigma_{LSJ}(\theta)\,, \tag{1}$$

where J_A and J_B are the spins of the target and residual nuclei respectively; L, S, J, are the orbital, spin, and total angular momentum transferred to the target nucleus, and $\sigma_{LSJ}(\theta)$ is the DWBA cross section. All angular momenta are related by the obvious selection rules for one-step "single-particle" transfer. If both ^{27}Al and ^{29}Si are deformed in their ground states an additional selection rule is present:

$$J\geq\Omega\,,\quad \Omega=|k_B-k_A|\,, \tag{2}$$

where Ω, k_B, and k_A are the projections of J, J_B, and J_A on the symmetry axis of the corresponding nuclei. This restriction will suppress some al-

TABLE II. Optical-model parameters used in analysis of ^{27}Al(α,d)^{29}Si [strengths in MeV, lengths in (fm)].

Label	Channel	V	r_0	a	W	$W'=4W_d$	r_0'	a'
K [a]	^{27}Al + α	196.5	1.30	0.630	24.3	0	1.30	0.63
K [b]	^{29}Si + d	102.5	1.175	0.585	0	88.0	1.25	0.68
K	d bound state	varied	1.175	0.400				
$A5$ [c]	^{27}Al + α	228.0	1.366	0.557	23.3	0	1.242	0.557
$D1$ [c]	^{29}Si + d	98.1	1.127	0.848	0	59.5	1.394	0.655
	bound state [d]	varied	1.260	0.600				

[a] Reference 10.
[b] Reference 11.
[c] Reference 12.
[d] Included Thomas spin orbit with $\lambda = 25$.

lowed L transfers if the strong-coupling model is important for the description of the excited states of ^{29}Si. It has been suggested[7] that the low-lying levels of ^{29}Si may be explained as members of three rotational bands: (1) $K^\pi = \frac{1}{2}^+$ band (Nilsson orbital 9) containing the g.s.($\frac{1}{2}^+$), 2.028-MeV($\frac{5}{2}^+$) and 2.425-MeV($\frac{3}{2}^+$) states; (2) $K^\pi = \frac{3}{2}^+$ band (Nilsson orbital 8) containing the 1.273-MeV($\frac{3}{2}^+$), 3.067-MeV ($\frac{5}{2}^+$) and 4.080-MeV($\frac{7}{2}^+$) states; and (3) $K^\pi = \frac{7}{2}^-$ band (Nilsson orbital 10) containing the 3.623-MeV($\frac{7}{2}^-$) level. Under these assumptions, $L = 0$ transfer is prohibited for the 2.028-MeV($\frac{5}{2}^+$) and the 2.425-MeV ($\frac{3}{2}^+$) states if we assume $K^\pi = \frac{5}{2}^+$ for the ground state of ^{27}Al.

TABLE III. Two-nucleon transfer amplitudes for ^{27}Al $\rightarrow$ ^{29}Si (Ref. 13). The symbols d, s, d' denote $1d_{5/2}$, $2s_{1/2}$, and $1d_{3/2}$, respectively.

E_x	J^π	J	d^2	s^2	d'^2	ds	dd'	sd'
0.0	$\frac{1}{2}^+$	2	0	0	0	+0.7532	0.0327	+0.1780
		3	0.3549	0	−0.0359	−0.7481	0.0798	0.0
1.27	$\frac{3}{2}^+$	1	−0.1766	−0.3600	0.0752	0	0.3704	−0.0515
		2	0	0	0	+0.0485	−0.5136	+0.1474
		3	−0.0613	0	−0.0416	+0.0371	0.6107	0
		4	0	0	0	0	−0.7022	0
2.03	$\frac{5}{2}^+$	1	−0.1267	0.3287	−0.0568	0	0.0047	+0.0121
		2	0	0	0	−0.1623	0.0459	−0.1146
		3	−0.1819	0	0.0050	+0.0178	0.0023	0
		4	0	0	0	0	0.0027	0
		5	−0.3436	0	0	0	0	0
2.43	$\frac{3}{2}^+$	1	−0.0890	−0.4918	0.0600	0	−0.0697	+0.1517
		2	0	0	0	−0.0306	0.1345	−0.3153
		3	0.0165	0	0.0227	+0.0729	−0.2076	0
		4	0	0	0	0	0.0765	0
3.07	$\frac{5}{2}^+$	1	0.0132	0.2834	−0.0599	0	0.1022	−0.2207
		2	0	0	0	−0.0630	−0.0534	+0.3063
		3	−0.0921	0	−0.0464	−0.0513	0.0406	0
		4	0	0	0	0	0.0948	0
		5	−0.1169	0	0	0	0	0
4.08	$\frac{7}{2}^+$	1	−0.0166	0.0144	0.0750	0	0.0429	+0.1463
		2	0	0	0	−0.0366	−0.0762	−0.2449
		3	−0.0180	0	0.0986	+0.0160	0.0773	0
		4	0	0	0	0	−0.1107	0
		5	0.0168	0	0	0	0	0

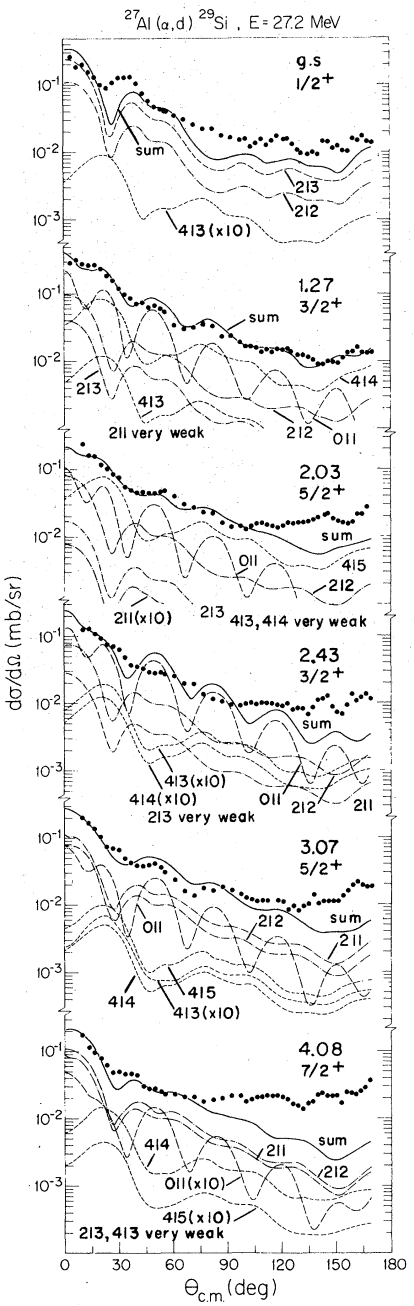

FIG. 3. Same as Fig. 2 but compared with microscopic DWBA curves calculated with potential set *A*5, *D*1 of Table II. Curves are labeled with *LSJ* values.

The reduced differential cross section $\sigma_{LSJ}(\theta)$ was computed with a computer code.[8] The factors A_{LSJ} in Eq. (1) are related to the "spectroscopic" factors S_{LJ} of the quasideuteron states in the final nucleus: $|A_{LSJ}|^2 \propto S_{LJ}$.

Initially, the sensitivity of the DWBA calculation to the choice of parameters was studied. These parameters are the geometrical parameters of the bound state of the quasideuteron in the residual nucleus and the optical potentials in the entrance and exit channels. The ground state transition is most favorable for this investigation: (1) The oscillatory pattern is more pronounced than in the other states, and (2) the number of different angular momentum transfers allowed is smaller than for the other states (Table I). The bound-state wave function was calculated in a Woods-Saxon potential well with the assumption that the transferred neutron and proton are moving as a single body (quasideuteron) with principle quantum number N and orbital angular momentum L. These quantities are related by $N=\frac{1}{2}(4-L)$ if we consider only the $2s$-$1d$ orbitals in ^{29}Si.[9]

The depth of the bound state potential well was found by requiring that the binding energy ϵ_d of the quasideuteron in the state of excitation energy E_i^* be equal to the separation energy B_c of a deuteron from that state of ^{29}Si. This requirement is not sufficient to determine a unique set of parameters V, r_0, and a, but rather defines an infinite set of bound-state potentials. The depth of the potential V_0 is strongly dependent on r_0 and weakly related to a. The choice of these parameters substantially influences the shape of the theoretical angular distributions. This fact was used to determine empirically r_0 and a. The best fit to the ground state angular distribution was found for $r_0=1.175$ fm and $a=0.40$ fm. The angluar distributions for the other states were then analyzed with the same bound-state geometry.

A four-parameter Woods-Saxon potential, with volume absorption, was used for the entrance channel. The parameters V, W, r_0, and a were found from an analysis[10] of the elastic scattering of 27.2 MeV alpha particles on ^{27}Al and are listed in Table II. The deuteron potential is from Ref. 11. Results of these DWBA calculations are shown in

TABLE IV. Normalization factors from microscopic DWBA calculations.

E_x (MeV)	J^π	$N(\times 10^{-3})$ Shell model	Weak coupling
0.00	$\frac{1}{2}^+$	8.4	8.4
1.27	$\frac{3}{2}^+$	11	27
2.03	$\frac{5}{2}^+$	20	6.6
2.43	$\frac{3}{2}^+$	10	4.5
3.07	$\frac{5}{2}^+$	23	7.8
4.08	$\frac{7}{2}^+$	39	13

TABLE V. Weak coupling amplitudes for ^{27}Al → ^{29}Si.

E_x (MeV)	J^π	Assumed configuration	J	Amplitudes
0	$\frac{1}{2}^+$	$0^+\otimes 2s_{1/2}$	2	$-0.6455(1d_{5/2})(2s_{1/2})$
			3	$0.7638(1d_{5/2})(2s_{1/2})$
1.27	$\frac{3}{2}^+$	$0^+\otimes 1d_{3/2}$	1	$-0.3536(1d_{5/2})(1d_{3/2})$
			2	0.4564
			3	−0.5401
			4	0.6124
2.03	$\frac{5}{2}^+$	$2^+\otimes 2s_{1/2}$	1	$0.6416(2s_{1/2})^2 - 0.3118(1d_{3/2})(2s_{1/2})$
			2	$0.4409(1d_{3/2})(2s_{1/2})$
2.43	$\frac{3}{2}^+$	$2^+\otimes 2s_{1/2}$	1	$0.8400(2s_{1/2})^2 + 0.3572(1d_{3/2})(2s_{1/2})$
			2	$0.4050(1d_{3/2})(2s_{1/2})$
3.07	$\frac{5}{2}^+$	$2^+\otimes 1d_{3/2}$	1	$-0.4850(2s_{1/2})(1d_{3/2}) - 0.2422(1d_{3/2})^2$
			2	$0.6859(2s_{1/2})(1d_{3/2}) - 0.0589(1d_{3/2})^2$
			3	$0.4107(1d_{3/2})^2$
4.08	$\frac{7}{2}^+$	$2^+\otimes 1d_{3/2}$	1	$0.0(2s_{1/2})(1d_{3/2}) + 0.2041(1d_{3/2})^2$
			2	$0.5144(2s_{1/2})(1d_{3/2}) - 0.3535(1d_{3/2})^2$
			3	$0.0(2s_{1/2})(1d_{3/2}) + 0.3535(1d_{3/2})^2$

Fig. 2.

The macroscopic selection rules for the ground state permit the transfer of two values of angular momentum, $L=2$ and $L=4$. However, the contribution of $L=4$ to this transition is found to be negligible and the ground state can be fitted by a pure $L=2$ distribution.

In contrast to the ground state, the excited states can be fitted only by mixing different L values. The theoretical distributions for $L=0$ and $L=4$ have oscillations which are out of phase with the $L=2$ distribution so that their mixing produces a relatively smooth curve in accordance with the data (Fig. 2). For angles $\leq 70°$ (c.m.) the fit is good for levels of the supposed ground state rotational band ($K=\frac{1}{2}$). The transitions corresponding to the $K=\frac{3}{2}$ band [1.273($\frac{3}{2}^+$), 3.067($\frac{5}{2}^+$), and 4.080($\frac{7}{2}^+$)] are not fitted as well at forward angles, possibly indicating a different bound-state geometry for each rotational band. The back angles are consistently underpredicted by DWBA with the difference increasing with increasing angle. If one assumes that this is due to compound nucleus contributions exclusively, then the compound reaction contribution for the ground state and six excited states would be 41%, 36%, 52%, 47%, 54%, 58%, and 78%, respectively. This very crude estimate from the integrated cross sections should be regarded as an upper limit only.

Among all of the excited states studied only the 3.623 MeV level has negative parity ($\frac{7}{2}^-$). The angular distribution of this state looks very similar to the data for the $\frac{7}{2}^+$ 4.08 MeV state. This may be partially explained as the consequence of similarities in the forward angles of $L=2$ and 3 and L mixing. For the mixing of $L=1$, 3, and 5 there is considerable discrepancy between the DWBA predictions and the experimental data for angles θ(c.m.) $\leq 20°$.

For the microscopic analysis, we have used the well-matched set of optical model parameters $D1$-$A5$ from Ref. 12 (in order to minimize finite-range effects), and two nucleon transfer amplitudes from a shell-model calculation. These amplitudes (Table III) have given a reasonable account of data for the ^{27}Al(^{3}He,p)^{29}Si reaction.[13] Cross sections were calculated with the two nucleon transfer options of the code DWUCK,[14] using the half-separation energy technique for binding energies. Experimental cross sections were related to theoretical ones through the expression

$$\sigma_{\text{exp}}(\theta) = N \frac{2J_f+1}{2J_i+1} \sum_{LJ} \frac{\sigma_{\text{DWBA}}(\theta)}{2J_x+1} .$$

Theoretical curves for different LJ transfer were added together in the ratio required by the shell-model amplitudes, and the summed cross section then arbitrarily normalized to the data (Fig. 3) to get the normalization factors, N, listed in Table IV. The fits are generally quite good. They underestimate the back-angle cross sections, but not to such an extent as the cluster calcula-

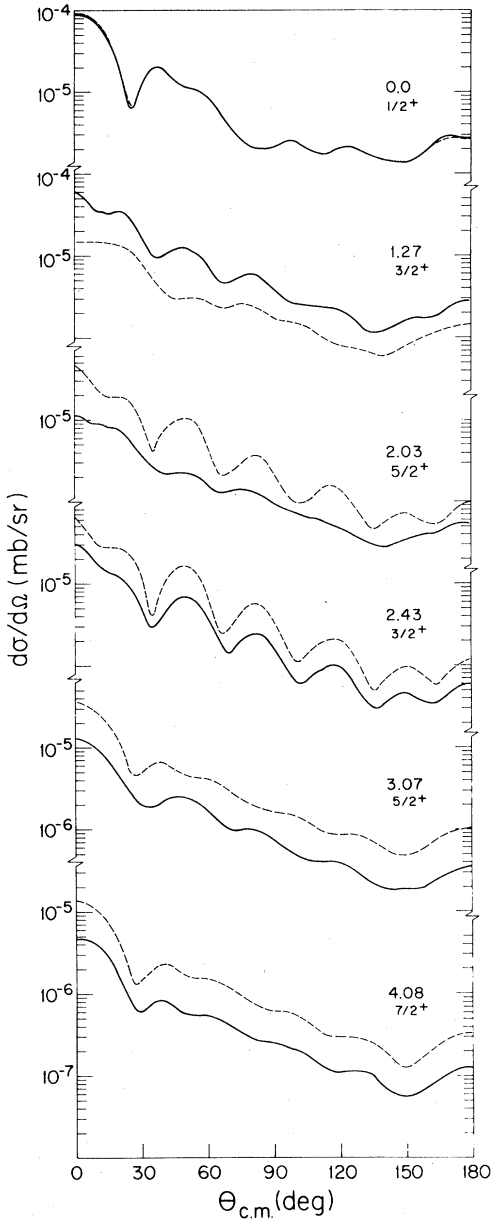

FIG. 4. Theoretical angular distributions for ^{27}Al(α,d), using two-nucleon transfer amplitudes from shell model (solid) and weak coupling (dashed).

tions.

We have also calculated transfer amplitudes in a weak-coupling picture, in which states of ^{29}Si are considered to be neutron single-particle states weakly coupled to the ground and first excited states of ^{28}Si. For ^{27}Al→^{28}Si(0^+), the amplitude is pure $1d_{5/2}$, whereas for ^{27}Al→^{28}Si(2^+), it is a mixture of $l=0(2s_{1/2})$ and $l=2$ (assumed $1d_{3/2}$). For these amplitudes we use the ratio of $l=0$ to $l=2$ spectroscopic factors measured[15] in ^{27}Al(d,n)^{28}Si(2^+):

$$\frac{S(l=0)}{S(l=2)}=2.4\,,$$

giving $A(2s_{1/2})=0.84$, $A(1d_{3/2})=0.54$. Resulting two-nucleon amplitudes are displayed in Table V.

This is probably not a good description of the states of ^{29}Si. In fact, the transfer amplitudes calculated from weak coupling (Table V) show marked differences from the shell-model ones (Table III). Nevertheless, the calculated cross sections for the two sets of amplitudes are remarkably similar (Fig. 4). It thus appears that a weak coupling description contains most of the essential features.

Finally we have computed cluster transfer spectroscopic factors from the microscopic two-nucleon amplitudes using SU(3) coefficients[16] listed in Table VI. These cluster spectroscopic factors are compared with those extracted from the cluster-transfer analysis in Table VII. Except for certain $L=4$ transfers, the ratio of experimental to theoretical spectroscopic factors is roughly constant at about 8 plus or minus about a factor of two. The large deviations for $L=4$ may be connected with the fact that this shell-model calculation does not correctly reproduce the degree of a $1d_{5/2}$ shell closure at ^{28}Si.

Finally, in Fig. 5, we display the experimental angular distribution for the $\frac{7}{2}^-$ state at 3.62 MeV, and microscopic DWBA curves for $L=1$, 3, and

TABLE VI. Cluster-transfer amplitudes.

J	$(nlj)_1(nlj)_2$	Amplitude $L=0$, $S=1$	$L=2$, $S=1$	$L=4$, $S=1$
1	$(1d_{5/2})^2$	0.353	−0.189	0
	$(1d_{3/2})^2$	−0.189	0.353	0
	$(1d_{5/2})(1d_{3/2})$	−0.533	−0.249	0
	$(2s_{1/2})(1d_{3/2})$	0	−0.882	0
	$(2s_{1/2})^2$	0.745	0	0
2	$(1d_{5/2})(2s_{1/2})$	0	0.558	0
	$(2s_{1/2})(1d_{3/2})$	0	0.683	0
	$(1d_{5/2})(1d_{3/2})$	0	0.471	0
3	$(1d_{5/2})^2$	0	0.370	−0.151
	$(1d_{3/2})^2$	0	−0.062	0.907
	$(1d_{5/2})(1d_{3/2})$	0	−0.285	−0.393
	$(1d_{5/2})(2s_{1/2})$	0	0.882	0
4	$(1d_{5/2})(1d_{3/2})$	0	0	1.0
5	$(1d_{5/2})^2$	0	0	1.0

TABLE VII. Comparison of theoretical and experimental cluster spectroscopic factors for $^{27}Al(\alpha,d)^{29}Si$.

E_x	J^π	L	S	J	S_{LSJ}(th) [a]	S_L(th) [b]	S_L(exp) [c]	R [d]
0.0	$\frac{1}{2}^+$	2	1	2	0.2776	0.8715	4.28	4.91
		2	1	3	0.5939			
		4	1	3	0.0138	0.0138	0.0	
1.27	$\frac{3}{2}^+$	0	1	1	0.2940	0.2940	0.90	3.06
		2	1	1	0.0061			
		2	1	2	0.1368	0.1944	1.62	8.33
		2	1	3	0.0515			
		4	1	3	0.0720			
		4	1	4	0.4931	0.5651	0.44	0.78
2.03	$\frac{5}{2}^+$	0	1	1	0.0435	0.0435		
		2	1	1	0.0002			
		2	1	2	0.0363	0.0436	0.48	11.01
		2	1	3	0.0071			
		4	1	3	0.0010			
		4	1	4	0.0	0.1191	2.76	23.17
		4	1	5	0.1181			
2.43	$\frac{3}{2}^+$	0	1	1	0.1385	0.1385		
		2	1	1	0.0358			
		2	1	2	0.0875	0.1233	0.71	5.76
		2	1	3	0.0			
		4	1	3	0.0099			
		4	1	4	0.0059	0.0158	2.70	171
3.07	$\frac{5}{2}^+$	0	1	1	0.0302	0.0302	0.41	13.58
		2	1	1	0.0592			
		2	1	2	0.0397	0.0989	0.89	9.00
		2	1	3	0.0			
		4	1	3	0.0019			
		4	1	4	0.0090	0.0246	0.31	12.6
		4	1	5	0.0137			
4.08	$\frac{7}{2}^+$	0	1	1	0.0010	0.001	0.0	
		2	1	1	0.0219			
		2	1	2	0.0230	0.043	0.70	14.80
		2	1	3	0.0024			
		4	1	3	0.0038			
		4	1	4	0.0123	0.0164	1.16	70.7
		4	1	5	0.0003			

[a] $S_{LSJ}(\text{th}) = \left| \sum_{(j_1 j_2)} C_{(j_1 j_2) \to LSJ} a_{(j_1 j_2)} \right|^2$.

[b] $S_L(\text{th}) = \sum_J S_{LSJ}(\text{th})$.

[c] From Table I.

[d] $R = S_L(\text{exp})/S_L(\text{th})$.

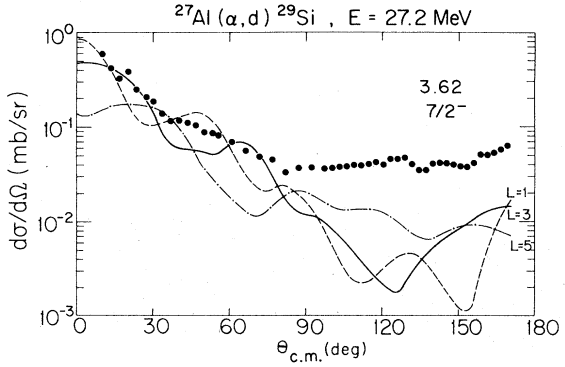

FIG. 5. Experimental angular distributions for the $\frac{7}{2}^-$ state at 3.62 MeV compared with microscopic DWBA curves for $L = 1$, 3, and 5.

5. A combination of the allowed L values can give a good account of the data up to about 90°, but for larger angles the DWBA curves fall below the data, as was the case for positive-parity states.

In conclusion, both cluster and microscopic DWBA calculations give reasonable accounts of the data for the reaction ^{27}Al(α,d), although both fail to account for all the measured back-angle cross sections. Two-nucleon transfer amplitudes calculated in weak coupling give results similar to those obtained from a shell-model calculation.

We wish to acknowledge financial support of the National Science Foundation. One of the authors (V. V. T.) is grateful for the support of a Fulbright-Hayes scholarship.

*On leave from Institute of Nuclear Research, Academy of Science of the Ukrainian SSR, Kiev, USSR.
[1]S. Kakigi, J. Phys. Soc. Jpn. 20, 1967 (1965).
[2]B. B. Srivastava and O. E. Johnson, Phys. Rev. 166, 1083 (1968).
[3]O. K. Gorpinich, Yu S. Stryuk, and V. V. Tokarevski, in *The Program and Abstracts of XXIII Meeting on Nuclear Spectroscopy and Atomic Nucleus Structure, Nauka, 1973*, p. 307.
[4]O. K. Gorpinich, Yu S. Stryuk, V. V. Tokarevski, and V. N. Shcherbin, Institute of Nuclear Research of the Academy of Science, Ukrainian Soviet Socialist Republic, Report No. KIYaI-76-37.
[5]V. V. Alekseev *et al.*, Izv. Akad. Nauk SSSR Ser. Fiz. 32, 1726 (1968).
[6]G. R. Satchler, Nucl. Phys. 55, 1 (1968).
[7]A. A. Pilt, R. H. Sper, R. V. Elliott, and J. A. Kuehner, Can. J. Phys. 49, 1263 (1971).
[8]V. V. Alekseev, V. N. Polanski, K. O. Terenetski *et al.*, Sizvestia AN USSR, Ser. Fiz. 34, 194 (1970).
[9]T. A. Brody and M. Moshinsky, Tables of Transformation Brackets, Mexico, 1960.
[10]Yu S. Stryuk and V. V. Tokarevski, in the Program and Abstracts of XXI Meeting of Nuclear Spectroscopy and Atomic Nucleus Structure, VII, Nauka, Leningrad, 1971, p. 85.
[11]Report of IF AN UKRSSR, Kiev, 1970, O. F. Nemets, editor.
[12]J. R. Comfort, H. T. Fortune, J. V. Maher, and G. C. Morrison, Phys. Rev. C 10, 2399 (1974).
[13]H. Nann, T. Mozgovoy, R. Bass, and B. H. Wildenthal, Nucl. Phys. A192, 417 (1972).
[14]P. D. Kunz (private communication).
[15]W. Bohne *et al.*, Nucl. Phys. A131, 273 (1969).
[16]M. De Llano *et al.*, Nucl. Phys. A72, 379 (1965).